
**ALTAIR05T-800 5 W wide range CV-CC optoless adapter
evaluation board**

Introduction

This application note describes the STEVAL-ISA176V1 evaluation board of the all primary-sensing switching regulator ALTAIR05T-800 and presents the results of its bench evaluation. The board implements a 5 W (5 V / 1 A) wide range mains battery charger with constant voltage/constant current.

The ALTAIR05T-800 combines a high-performance low-voltage PWM controller chip and an 800 V, avalanche rugged power MOSFET in the same package.

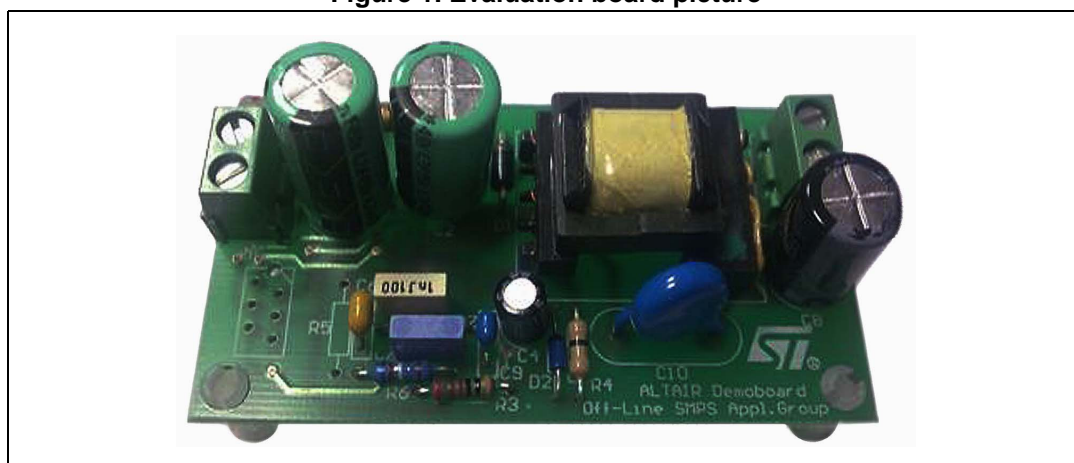
The PWM chip is a quasi-resonant (QR) current mode controller IC specifically designed for QR ZVS (zero-voltage switching at switch turn-on) flyback converters.

The device is capable of providing constant output voltage (CV) and constant output current (CC) regulation using primary sensing feedback. This eliminates the need for the optocoupler, the secondary voltage reference, as well as the current sensor, while maintaining very accurate regulation.

Additionally, it is possible to compensate the voltage drop of the output cable, so as to improve CV regulation on the externally accessible terminals.

Extremely low consumption under no-load conditions is ensured thanks to a controlled burst mode operation that, along with the built-in high-voltage startup circuit and the low operating current of the device, helps minimize residual input consumption. Although an auxiliary winding is required in the transformer to correctly perform CV/CC regulation, the chip is capable of powering itself directly from the rectified mains. This is useful especially during CC regulation, where the flyback voltage generated by the winding drops. However, if ultra low no-load input consumption is required to comply with the most stringent energy saving recommendations, then the device needs to be powered via the auxiliary winding.

Figure 1. Evaluation board picture



Contents

1	Test board: design and evaluation	3
2	Efficiency and no-load measurements	9
2.1	Standby optimization: tips for reducing standby consumption	10
2.1.1	Design optimization	11
2.2	Five star charger energy rating	12
3	Typical board waveforms	13
4	V-I output characteristics and cable drop compensation	17
5	Conclusion	20
Appendix A	Modes of operation	21
A.1	Constant voltage operation	21
A.2	Constant current operation	22
A.3	Current comparator speed	23
A.4	Cable drop compensation block	24
6	Revision history	26

1 Test board: design and evaluation

A 5 W battery charger evaluation board based on ALTAIR05T-800 is now presented. [Table 1](#) summarizes the electrical specifications of the application. [Table 2](#) provides the bill of materials and [Table 3](#) lists the transformer specifications. The electrical schematic is shown in [Figure 2](#) and the PCB layout in [Figure 3](#) and [Figure 4](#).

Table 1. ALTAIR05T-800 evaluation board: electrical specification

Parameter	Value
Input voltage range (V_{IN})	90 - 265 V _{AC}
Mains frequency (f_L)	50 - 60 Hz
Maximum (rated) output power	5 W
Output	$V_{OUT} = 5 \text{ V} \pm 5\%$ $I_{OUT} = 0 \text{ to } 1 \text{ A} \pm 7\%$ $V_{ripple} < 100 \text{ mV}$
Minimum switching frequency in normal mode	70 kHz
Target average efficiency (at $P_{OUT} = 5 \text{ W}$, $V_{IN} = 90 - 264 \text{ V}_{AC}$)	$> 70\%$ ⁽¹⁾
Maximum input power in standby	$< 100 \text{ mW}$ ⁽²⁾

1. Compliant with the EPA 2.0 standard for low voltage devices ($V_{OUT} < 6$, $I_{OUT} > 0.55 \text{ A}$).
2. Compliant with the European Code of Conduct, adapter for mobile handheld battery-driven applications, starting from 1st January 2011.

Figure 2. STEVAL-ISA176V1 electrical schematic

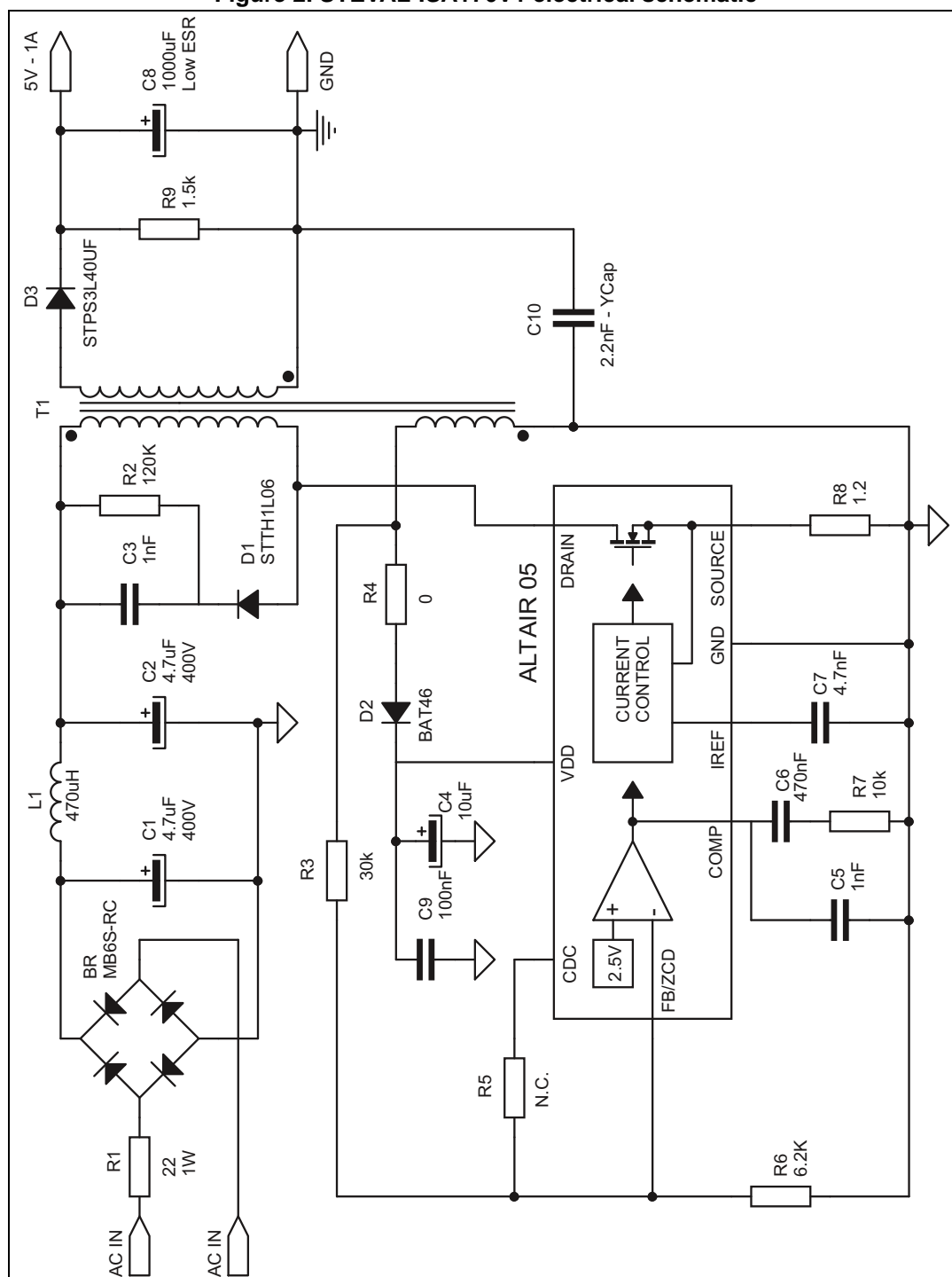


Table 2. ALTAIR05T-800 evaluation board: bill of material⁽¹⁾

Reference	Part	Description	Note
R1		22 Ω - 1 W	Axial flame proof
R2		120 k Ω SMD (1206)	
R3		36 k Ω	1% tolerance
R4		0 Ω	
R5		Not connected	See Section A.4: Cable drop compensation block
R6		7.5 k Ω	1% tolerance
R7		10 k Ω	
R8		1.2 Ω	1% tolerance
R9		1.5 k Ω	
C1, C2		4.7 μ F 400 V electrolytic	
C3		1 nF - 500 V XR7	
C4		10 μ F - 35 V electrolytic	
C5		1 nF - 25 V	
C6		470 nF - 25 V	
C7		4.7 nF - 25 V	
C8	B41889A4108M	1000 μ F - 16 V electrolytic	Epcos
C9		100 nF - 25 V	
C10	Y1- capacitor	2.2 nF - 230 V	
D1	STTH1L06	Ultra fast high voltage diode	STMicroelectronics
D2	BAT46	Small signal Schottky diode	STMicroelectronics
D3	STPS3L40UF	Power Schottky diode	STMicroelectronics
L1	B78108S1474J	470 μ H axial inductor	Epcos
BR	MB6S RC	Input bridge rectifier	
TF	1335.0032 rev.1	Flyback transformer	Magnetica®
IC	ALTAIR05T-800	Primary switching regulator	STMicroelectronics

1. If not otherwise specified, all resistors are 5%, 1/4 W.

Figure 3. PCB: top side and through-hole components(a)

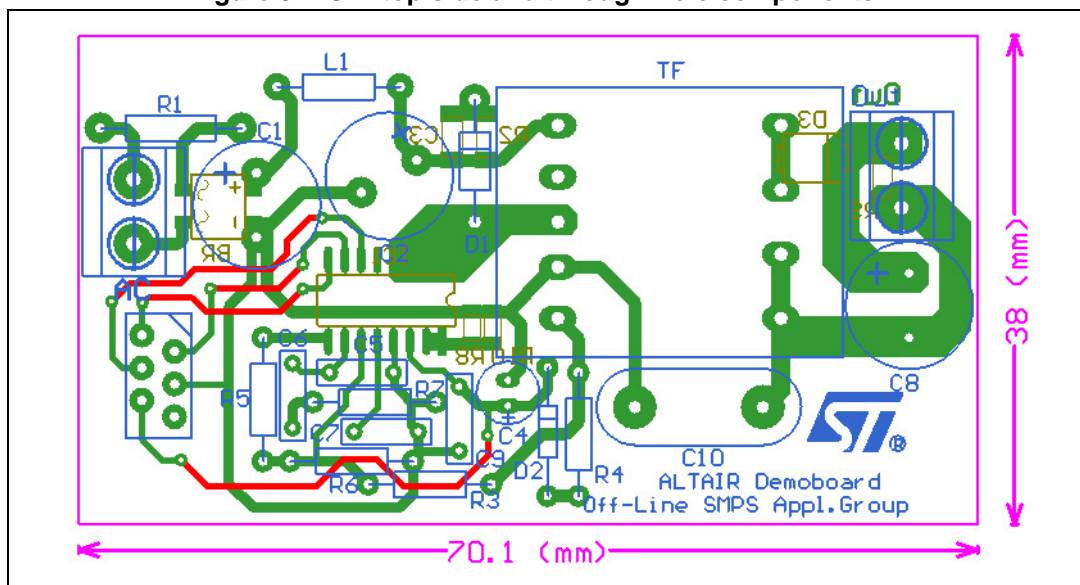
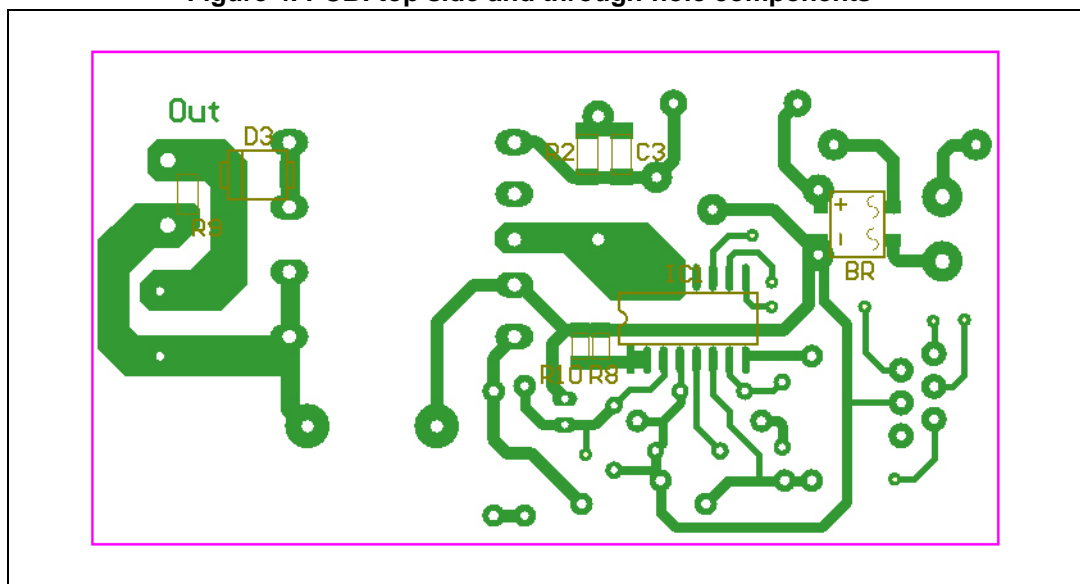


Figure 4. PCB: top side and through-hole components (a)

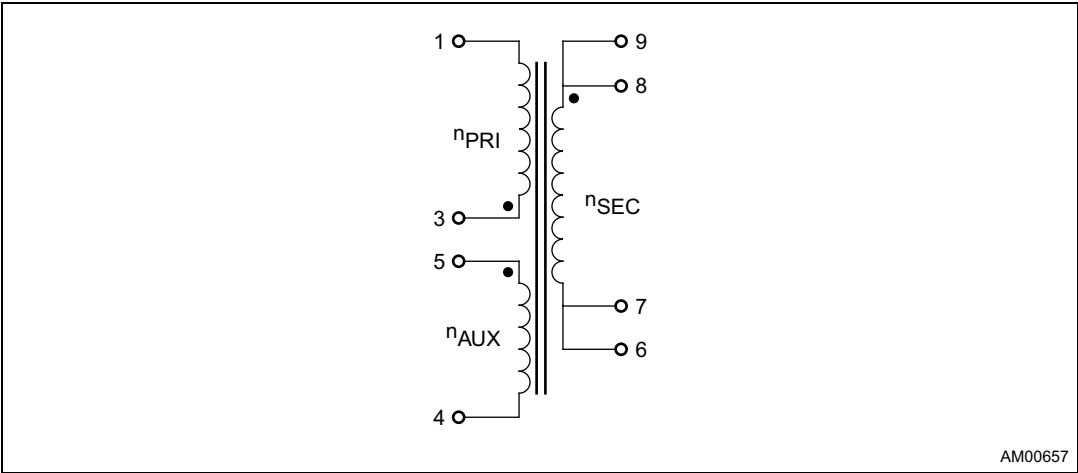


a. Layout is not to scale.

Table 3. ALTAIR05T-800 evaluation board: transformer characteristics

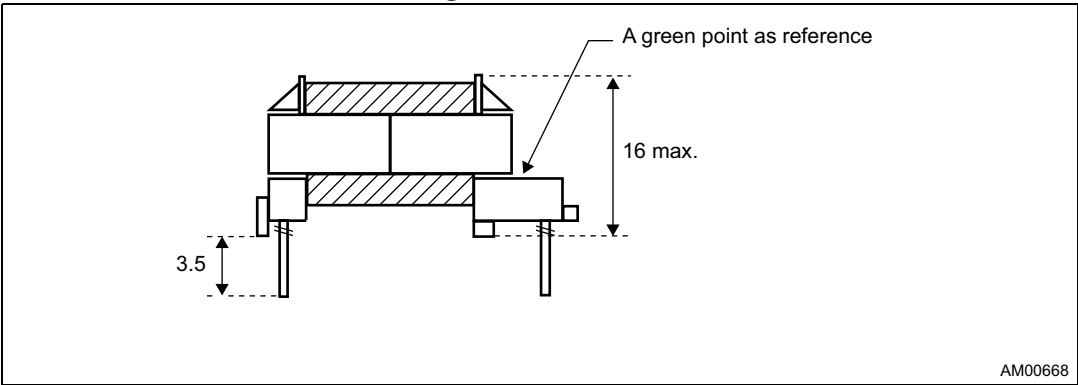
Name	Value
Manufacturer	Magnetica
Part number	1335.0032 rev. 1
Core	E16/5
Primary inductance	2.2 mH \pm 15%
Air gap	0.18 mm
Leakage inductance	66 μ H max.
Primary to secondary turn ratio	13.9 \pm 5%
Primary to auxiliary turn ratio	5 \pm 5%
Primary saturation current	0.4 A _P max. (B _{SAT} = 0.35 T)
Insulation primary to secondary	4 kV

Figure 5. Electrical schematic



AM00657

Figure 6. Side view



AM00668

Figure 7. Bottom side view

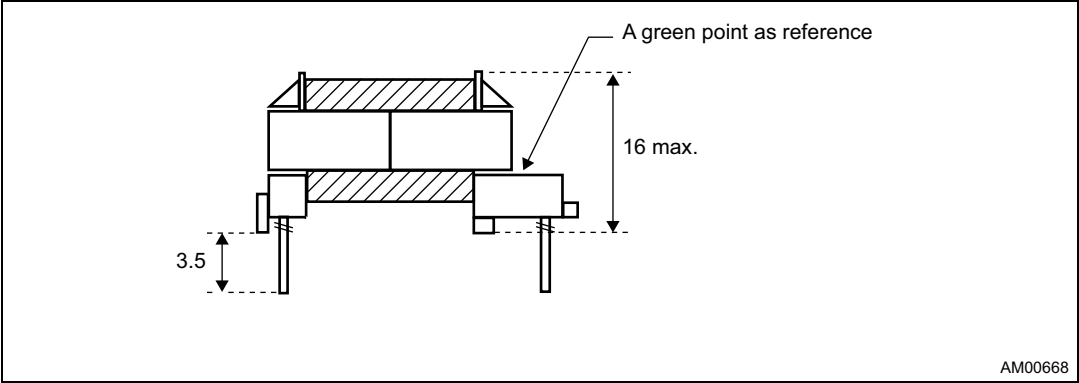
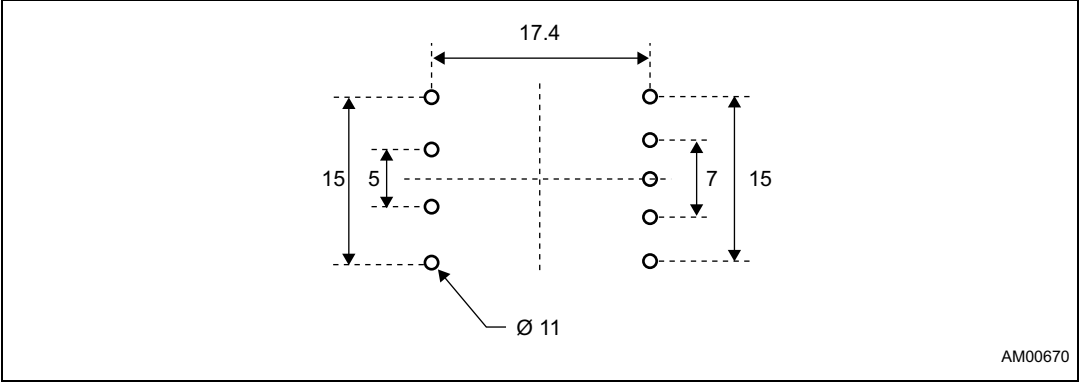


Figure 8. PCB hole dimensions



2 Efficiency and no-load measurements

The efficiency of the converter has been measured in different load and line voltage conditions.

According to the Energy Star average active mode testing efficiency method, the efficiency measurements have been performed at 25%, 50% and 75% and 100% of the rated output power, at both 115 V_{AC} and 230 V_{AC}.

Table 4 and Table 5 show the results.

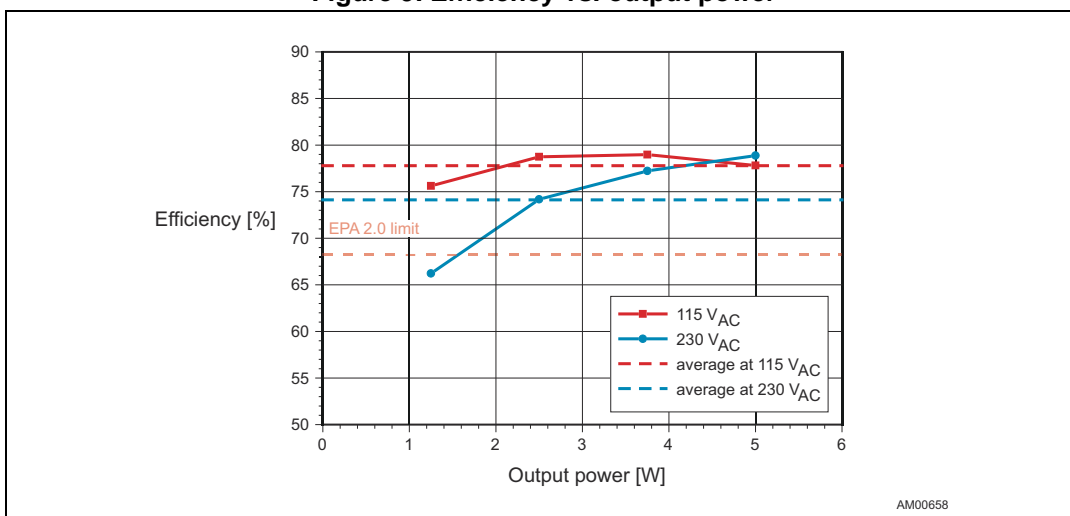
Table 4. Efficiency at 115 V_{AC}

Load [%]	I _{OUT} [A]	V _{OUT} [V]	P _{OUT} [W]	P _{IN} [W]	Efficiency [%]
25	0.25	4.97	1.243	1.643	75.62
50	0.5	4.97	2.485	3.156	78.74
75	0.75	4.97	3.728	4.72	78.97
100	1	4.98	4.980	6.4	77.81
Average efficiency					77.79

Table 5. Efficiency at 230 V_{AC}

Load [%]	I _{OUT} [A]	V _{OUT} [V]	P _{OUT} [W]	P _{IN} [W]	Efficiency [%]
25	0.25	4.98	1.245	1.88	66.22
50	0.5	4.97	2.485	3.349	74.18
75	0.75	4.98	3.735	4.838	77.22
100	1	4.99	4.99	6.326	78.88
Average efficiency					74.12

Figure 9. Efficiency vs. output power



This adapter complies with the new EPA 2.0 standard for low voltage devices ($V_{OUT} < 6$, $I_{OUT} > 0.55$ A). The minimum required efficiency for a 5 W SMPS is 68.2%. This value should be calculated as the average of the efficiency at 25%, 50%, 75% and 100% of the rated load.

The input power without load has also been measured and as indicated in [Table 6](#), for both 115 V_{AC} and 230 V_{AC}.

The proposed adapter using the ALTAIR05T-800 meets the most restrictive worldwide standards for efficiency and power consumption at no-load (European Code of Conduct, adapter for mobile handheld battery-driven applications, starting from 1st January 2011: < 150 mW).

Table 6. Standby consumption

V _{IN} [V]	P _{IN} [mW]
115 V _{AC}	54 mW
230 V _{AC}	75 mW

2.1 Standby optimization: tips for reducing standby consumption

When light loaded or in no-load condition, most of the losses are switching losses, which are almost proportional to the switching frequency. It should be considered that even if no external load is connected to the power supply, some power needs to be processed in order to sustain the operation of the ALTAIR05T-800 and some is also dissipated on the bleeder resistor at the secondary side.

Basically, when the converter switches to burst mode operation, the lower the load, the lower the average switching frequency. So, the burst mode operation of the ALTAIR05T-800 significantly reduces the average switching frequency of the converter, when light loaded or completely no-loaded.

As the output voltage is sensed through the auxiliary winding just at the end of the secondary demagnetization, rendering the IC is blind to the output voltage between one switching cycle and the next, the switching frequency cannot be reduced below the minimum restart time, $T_{RESTART}$, fixed at 500 μs (typical value).

Let's calculate the minimum input power consumption when the IC works at minimum restart frequency:

Equation 1

$$P_{IN(MIN)} = \frac{1}{2} \times L_P \times \left(\frac{V_{SENSE_M}}{R_{SENSE}} \right)^2 \times \frac{1}{T_{RESTART}}$$

where (V_{SENSE_M}/R_{SENSE}) is the peak drain current during burst mode ($V_{SENSE_M} = 140$ mV internally defined).

Neglecting the losses through the input bridge rectifier, the input capacitor leakage current losses and the conduction losses, the primary side losses can be calculated as follows:

Equation 2

$$P_{PRI} = P_{BIAS} + P_{SW} + P_{SNUBBER}$$

where $P_{BIAS} = V_{CC} \times I_Q$ is the consumption of the IC (the quiescent current, I_Q , is 1 mA typical value), P_{SW} represents the switching losses and $P_{SNUBBER}$ are the losses through the RCD snubber connected to the drain.

If $P_{IN(MIN)} > P_{PRI}$, the residual energy is transferred to the secondary side and it must be dissipated through a dummy load in order to avoid an increase in the output voltage. In this case, the bleeder resistor can be calculated as following:

Equation 3

$$R_{BLEEDER} \leq \frac{V_{OUT}^2}{\left[\frac{1}{2} \times L_P \times \left(\frac{V_{SENSE_M}}{R_{SENSE}} \right)^2 \times \frac{1}{T_{RESTART}} \right] - P_{PRI}}$$

However, if $P_{IN(MIN)} = P_{PRI}$ the dummy load can be removed.

Since most of the time P_{PRI} is lower than $P_{IN(MIN)}$, the above consideration shows that input power reduction can be achieved by reducing [Equation 1](#) so that the $R_{BLEEDER}$ can be increased in accordance with [Equation 3](#).

2.1.1 Design optimization

The sense resistor R_{SENSE} sets the constant current value together with transformer's primary-to-secondary turn ratio (see [Section A.2](#)), but also defines the minimum input power consumption according to [Equation 4](#).

A proper design can help reduce the energy per switching cycle transferred to the secondary and, consequently, no-load consumption. This can be done by increasing R_{SENSE} as much as possible and consequently, increasing the transformer's reflected voltage, in order to achieve the CC setpoint according to [Equation 4](#). Other design considerations should be taken into account in designing the transformer.

For the purpose of reducing the switching losses, some consideration should also be given to the transformer. The primary parasitic capacitance causes switch-on losses as it is fast-charged each time the MOSFET is turned on and the charging current dissipates energy within the MOSFET itself. Reducing this capacitance as low as possible, this type of loss is minimized.

With reference to [Equation 1](#), it is clear that a reduction of the $P_{IN(MIN)}$ can be achieved by reducing, as much as possible, the primary inductance of the transformer (L_P), (according to other design considerations also).

In this case the energy per cycle sent to the secondary side is reduced, which means that the bleeder resistor value increases, thus reducing the dissipation of the dummy load.

2.2 Five star charger energy rating

To help save energy, in November 2008 the world's five largest mobile phone makers announced their own five star energy rating system to help consumers more easily identify the most energy-efficient chargers.

The new rating system shows how much energy each charger uses when left plugged in. Chargers are labeled with ratings from five stars for the most efficient chargers ($\leq 0.03\text{ W}$), to zero stars for those using the most energy in no-load mode ($> 0.5\text{ W}$).

Figure 10. No-load consumption score chart

★★★★★	$\leq 0.03\text{W}$
★★★★	$> 0.03\text{W to } 0.15\text{W}$
★★★	$> 0.15\text{W to } 0.25\text{W}$
★★	$> 0.25\text{W to } 0.35\text{W}$
★	$> 0.35\text{W to } 0.5\text{W}$
No Stars	$> 0.5\text{W}$

As shown in [Table 6](#), the charger presented here meets the “**four star rating**”.

By optimizing the design, based on suggestions provided in [Section 2.1](#), the input power consumption can be reduced. Also, if a higher output voltage in no-load can be accepted, the bleeder resistor value can be increased a bit more than the minimum value in [Equation 3](#), thus achieving a further reduction in no-load consumption and helping to meet the “**five star rating**”.

3 Typical board waveforms

Drain voltage and current waveforms were reported for the two nominal input voltages and for the minimum and the maximum voltage of the converter input operating range. [Figure 11](#) shows the drain current and the drain voltage waveforms at nominal input voltages and full load.

In order to simulate this mode of operation, the electronic load has been set in CV mode at 3 V, so that this voltage is imposed on the charger's output from the E-load: the charger is forced to enter CC mode, thus regulating the output current at its nominal value. [Figure 12](#) shows the typical waveforms during CC mode.

The CC mode loop is able to regulate even when the output voltage falls to zero, thanks to the self-supply capability of the IC. This is especially important when the output connector is shorted. In this case, the current is still maintained close to the nominal value, thus eliminating hiccup mode and reducing the secondary peak current.

Moreover, the CC mode technique eliminates the need for overload protection. In fact, maximum output power is achieved on the corner point between CV mode and CC mode, and coincides with the full load condition. [Figure 13](#) shows the typical waveforms during short-circuit at nominal input voltage.

As described in [Section 2](#), at low load the OC enters in burst mode, reducing the switching frequency down to a minimum fixed value: [Figure 14](#) shows the typical waveforms during no-load conditions at both 115 V_{AC} and 230 V_{AC} circuit at nominal input voltage.

[Figure 15](#) and [Figure 16](#) show the charger startup in both no-load and full load conditions and nominal input voltage: the maximum drain-source voltage is well below the BV_{DSS} of the IC and the output voltage overshoot is always below 5.3 V.

Figure 11. Normal operation at full load, at 115 V_{AC} and 230 V_{AC}

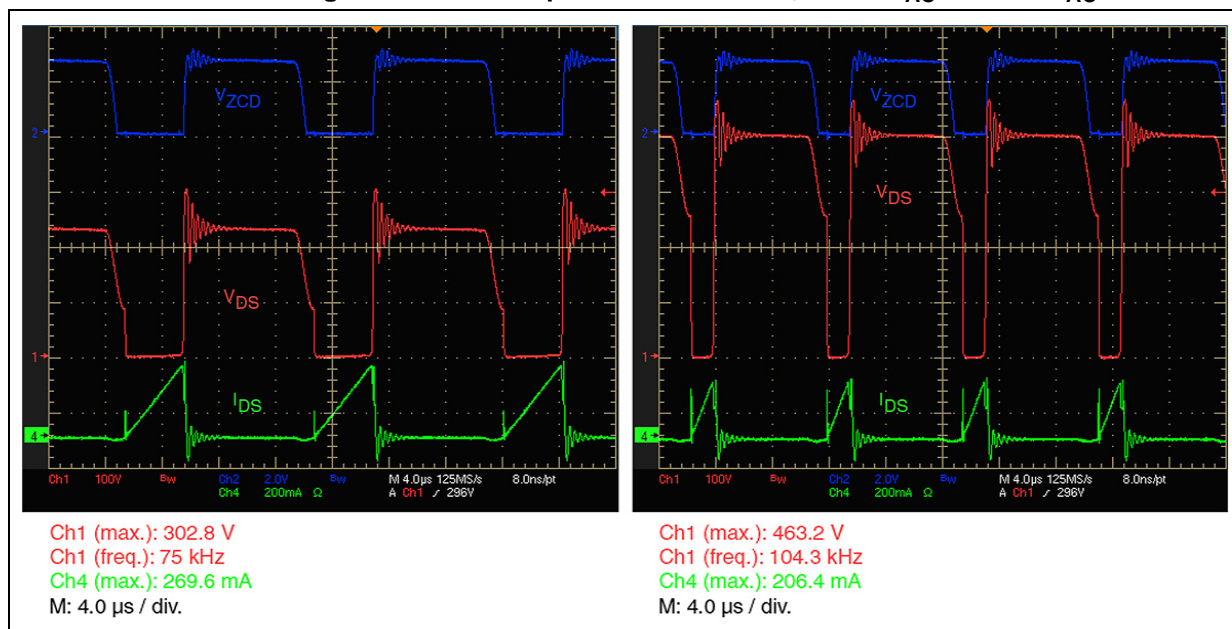


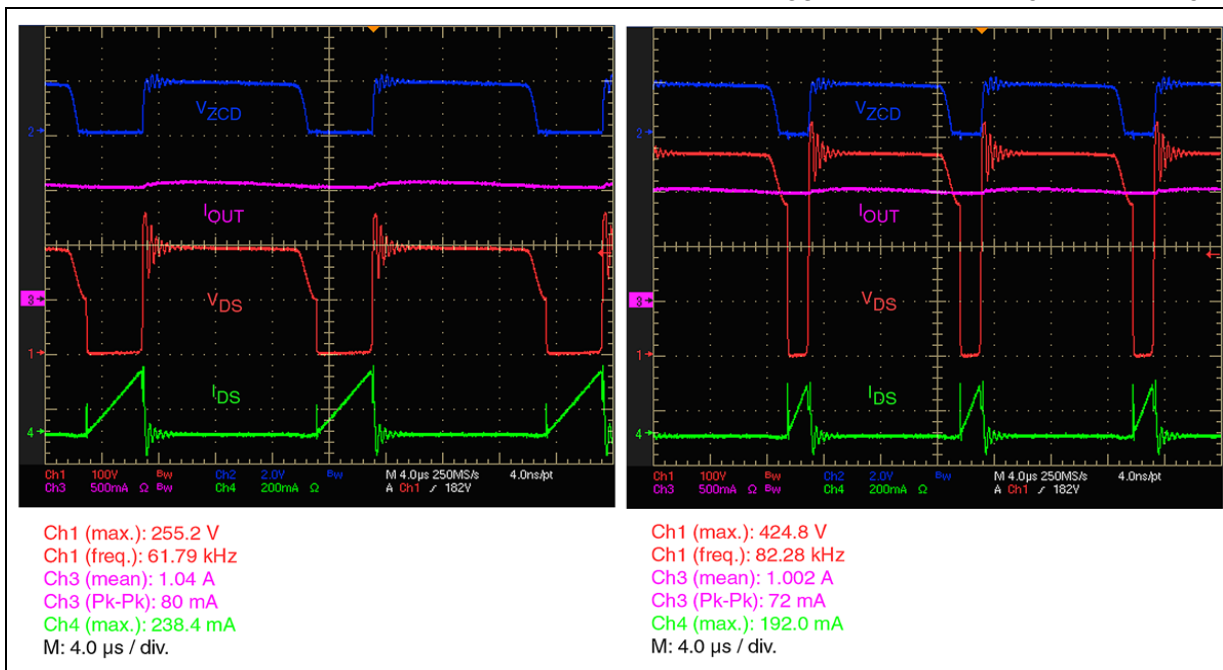
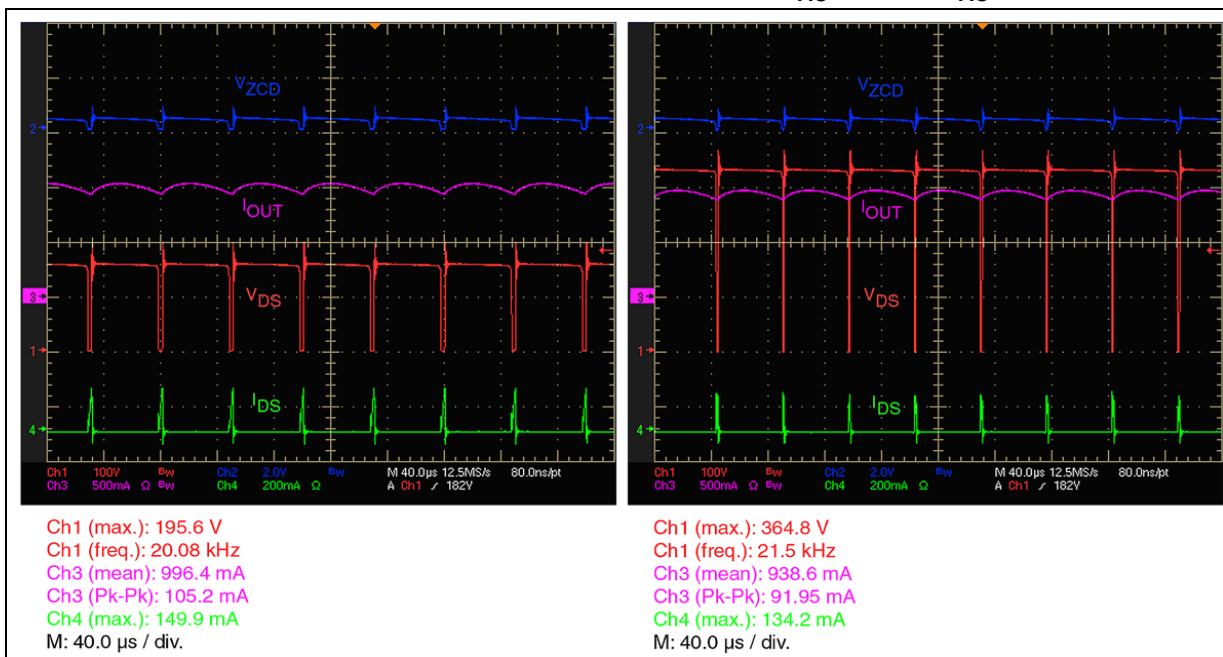
Figure 12. Normal operation in CC mode with $V_{OUT} = 3\text{ V}$, at 115 V_{AC} and 230 V_{AC} Figure 13. Short-circuit at 115 V_{AC} and 230 V_{AC} 

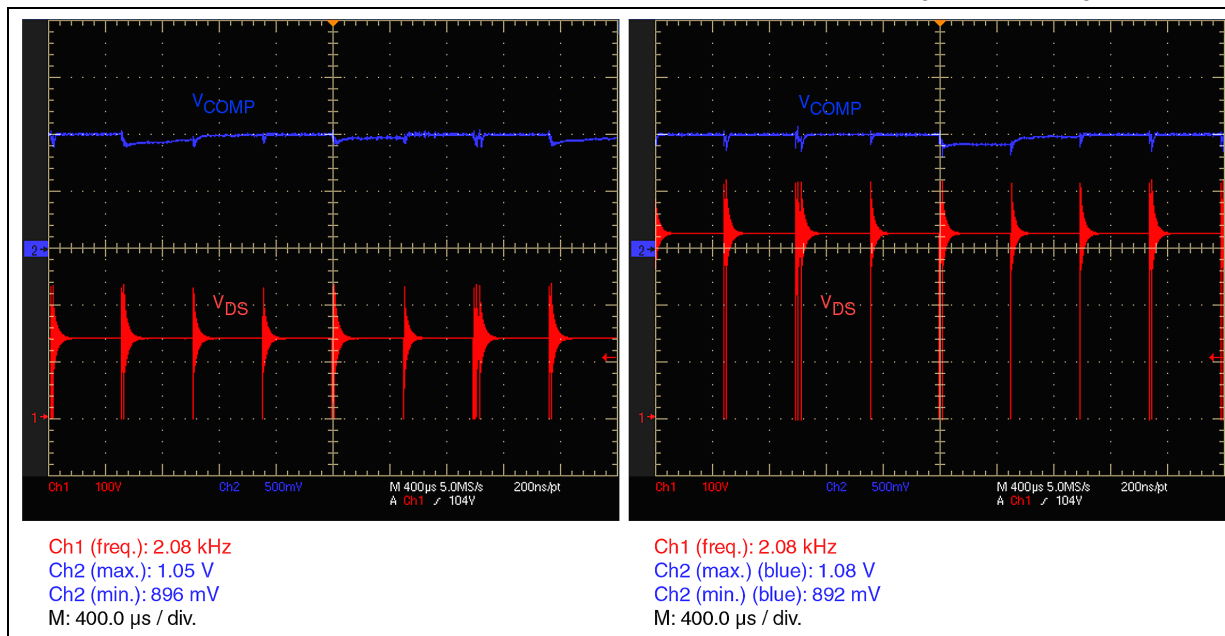
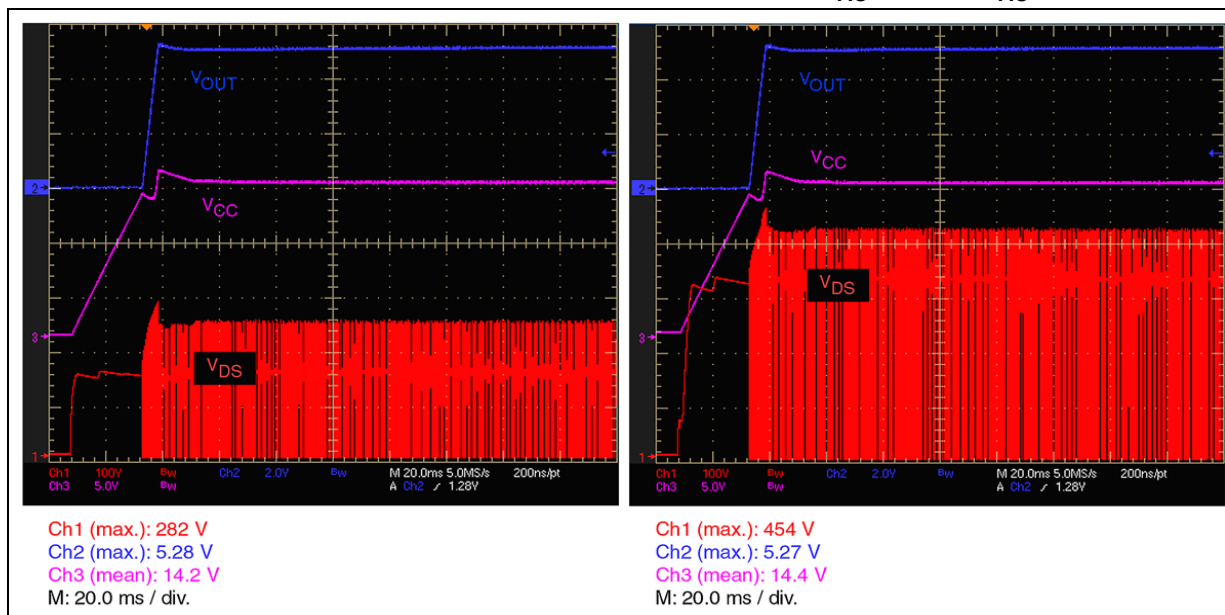
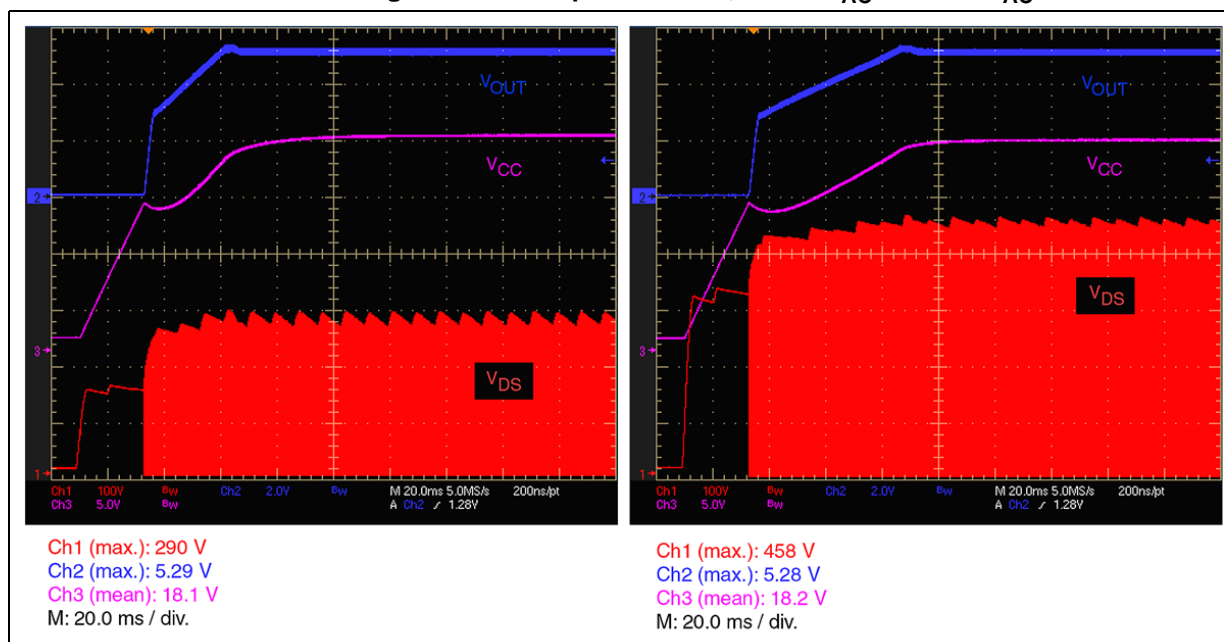
Figure 14. Normal operation at no-load, at 115 V_{AC} and 230 V_{AC}Figure 15. Startup at no-load, at 115 V_{AC} and 230 V_{AC}

Figure 16. Startup at full load, at 115 V_{AC} and 230 V_{AC}

4 V-I output characteristics and cable drop compensation

Figure 17 and *Figure 18* show the V-I output characteristics at the PCB output connector, measured at 115 V_{AC} and 230 V_{AC} mains input voltage.

Thanks to the self-supply of the ALTAIR05T-800, the output current can be regulated even with an output voltage close to zero.

The IC is also equipped with a cable compensation function that compensates the output voltage drop when a long cable is used, so ideally zero-load regulation can be achieved even at the end of the cable.

Figure 19 shows the load regulation in CV mode when the CDC function is not used: the voltage is tightly regulated at the end of the PCB connector, whereas at the end of the cable it decreases proportionally to the output current.

Conversely, in *Figure 20* the effect of the cable drop compensation is shown. The CV setpoint is increased proportionally to the output current, in order to compensate the voltage drop across the cable and maintaining the regulation at the end of the cable almost constant.

Figure 17. Output characteristic at 115 V_{AC}

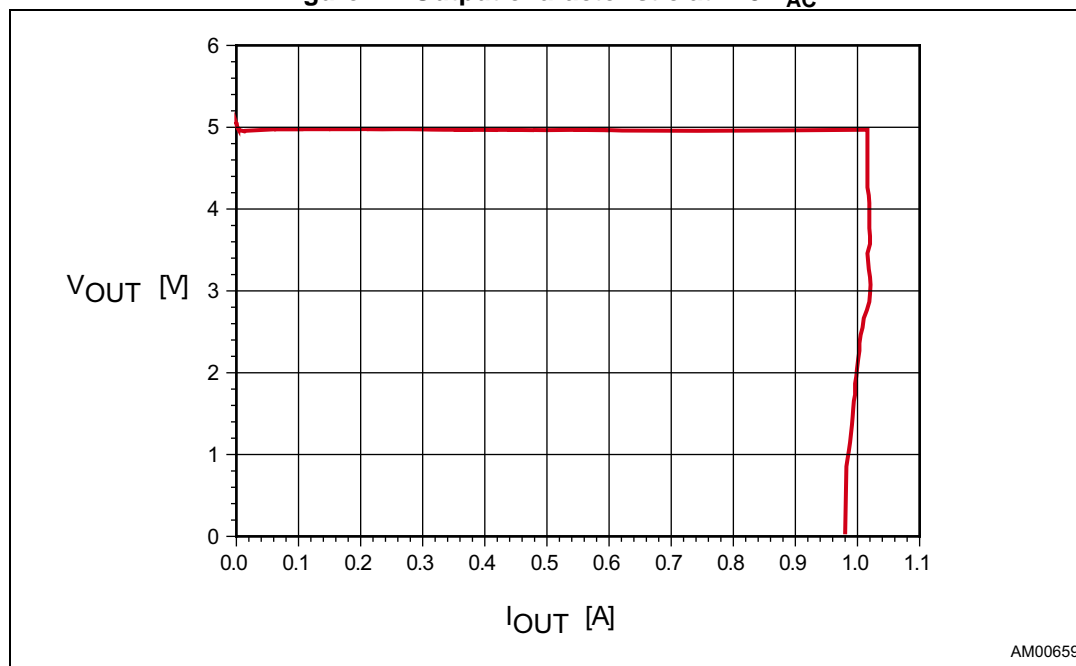


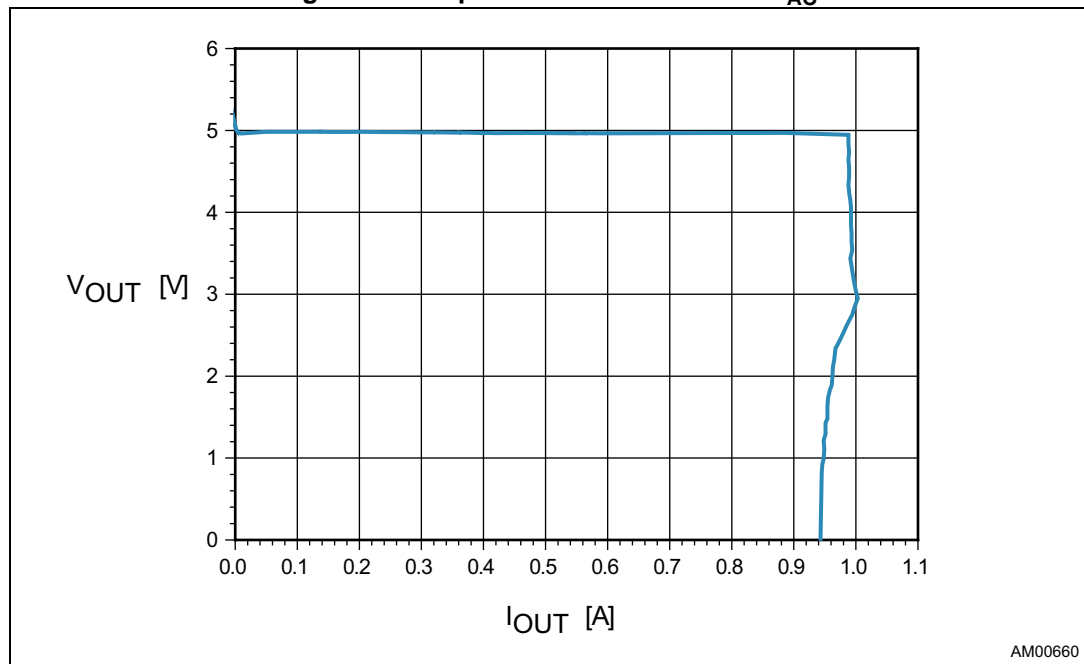
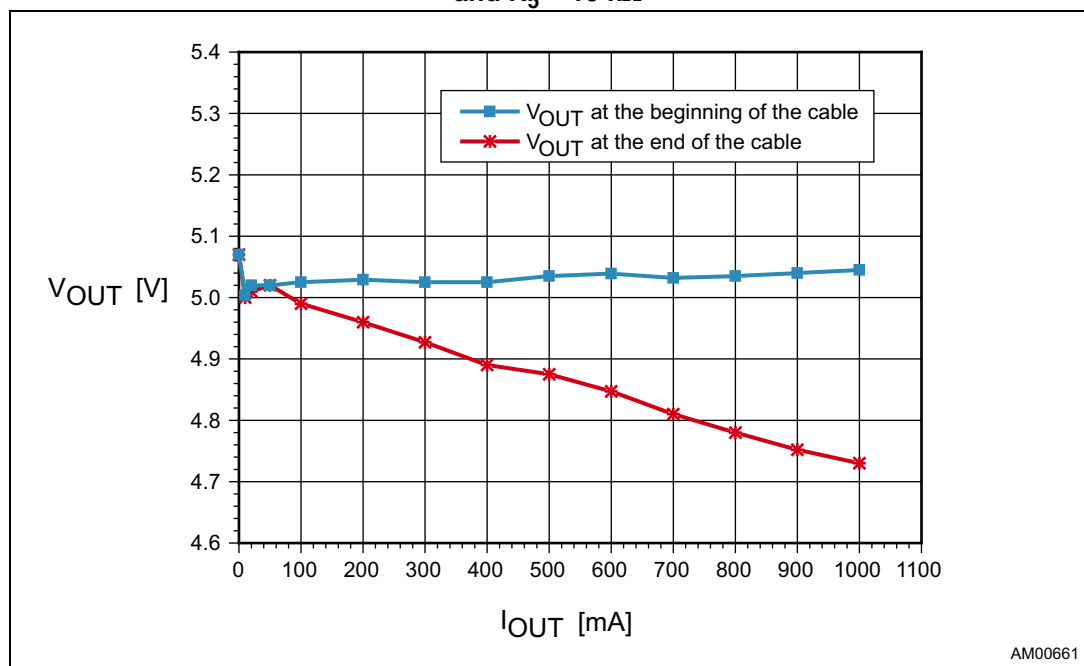
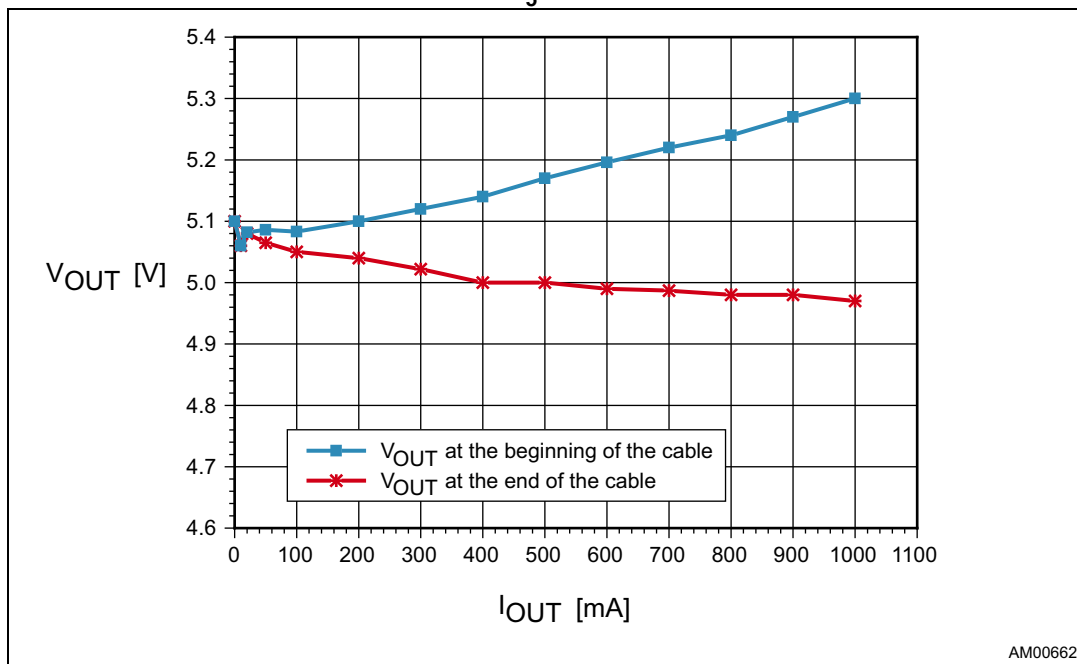
Figure 18. Output characteristic at 230 V_{AC}Figure 19. Output characteristic without cable drop compensation: $R_{CABLE} = 0.32 \Omega$ and $R_5 = 10 \text{ k}\Omega$ 

Figure 20. Output characteristic with cable drop compensation: $R_{\text{CABLE}} = 0.32 \, \Omega$ and $R_5 = 10 \, \text{k}\Omega$



5 Conclusion

A 5 W CV-CC optoless adapter evaluation board using the ALTAIR05T-800 device was presented and the results show that very good performance can be obtained using this new device.

The unique “all-primary sensing” feedback for both constant voltage and constant current eliminates the need for the optocoupler, the secondary voltage reference, as well as the current sensor, making the IC suitable for AC-DC chargers for mobile phones and other portable equipment, as well as any adapter requiring tight tolerance from both CV and CC regulation.

The ALTAIR05T-800 is capable of meeting the most restrictive worldwide standards for efficiency and power consumption at no-load.

The embedded protection features of this new device and the 800 V power section considerably increase the safety and reliability of the end product.

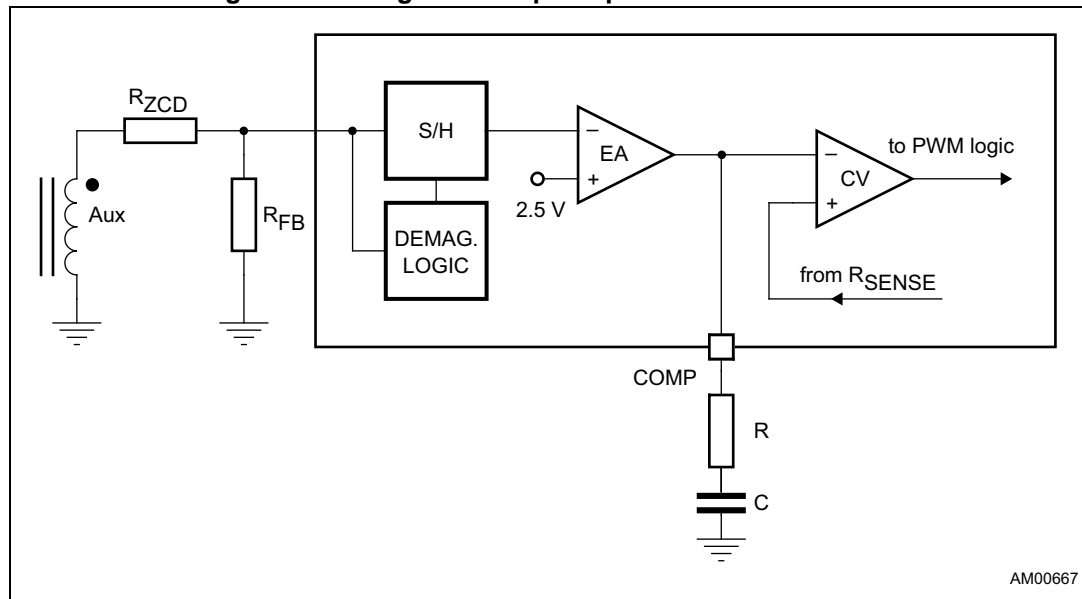
Appendix A Modes of operation

A.1 Constant voltage operation

The IC is specifically designed to work in primary regulation and the output voltage is sensed through a voltage partition of the auxiliary winding, just before the auxiliary rectifier diode.

[Figure 21](#) shows the internal schematic of the constant voltage mode and the external connections.

Figure 21. Voltage control principle: internal schematic



In order to achieve a tight output regulation, the signal on the ZCD/FB pin is sampled and held at the end of the transformer demagnetization to obtain an accurate image of the output voltage, and it is compared with the error amplifier internal reference.

The internal error amplifier delivers an output current proportional to the voltage imbalance of the two outputs: the output generates the control voltage that is compared with the voltage across the sense resistor, thus modulating the cycle-by-cycle peak drain current.

The output voltage can be set by choosing R_{FB} according to [Equation 4](#):

Equation 4

$$R_{FB} = \frac{V_{REF}}{\frac{n_{AUX}}{n_{SEC}} \times V_{OUT} - V_{REF}} \times R_{ZCD}$$

Where n_{SEC} and n_{AUX} are the secondary and auxiliary number of turns, respectively.

The R_{ZCD} value can be defined based on the application parameters and can be calculated according to [Equation 6](#).

A.2 Constant current operation

Figure 22 presents the principle used for controlling the average output current of the flyback converter.

The output voltage of an auxiliary winding is used by a demagnetization block to generate the control signal for the MOSFET switch Q1. A resistor (R) in series with it absorbs the current V_C/R , where V_C is the voltage developed by capacitor C_{REF} .

The flip-flop's output is high, as long as the transformer delivers current on the secondary side (Figure 23).

If the value of the capacitor (C) is sufficiently high to consider the voltage V_C as constant, and the system works in DCM (this is the case because the IC is in QR mode), it is possible to obtain the equation:

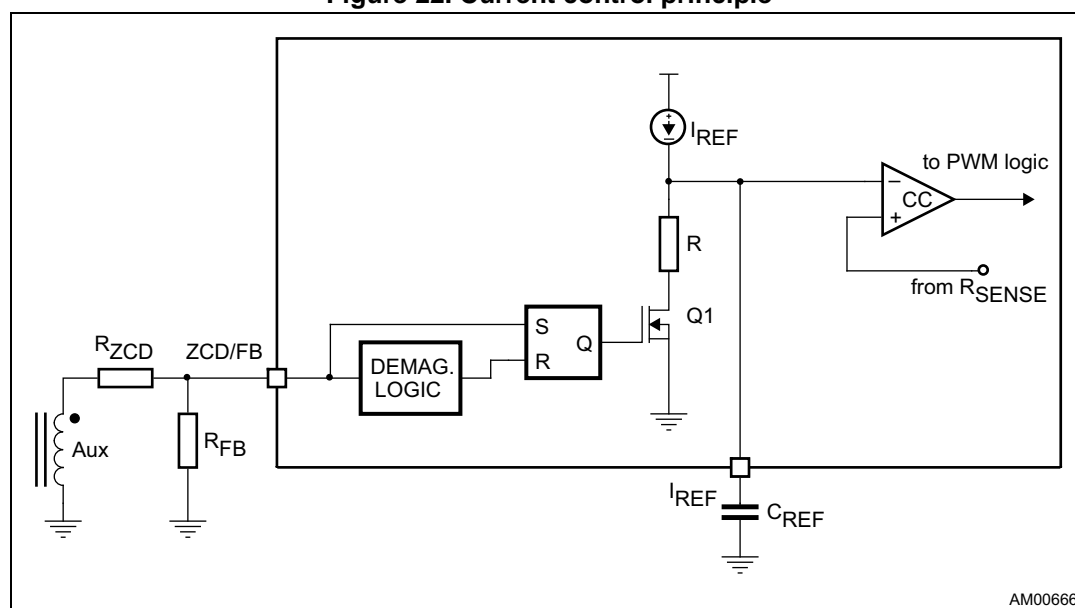
Equation 5

$$I_{OUT} = \frac{n}{2} \times \frac{V_{CREF}}{R_{SENSE}}$$

Where n is the primary-to-secondary turn ratio and $V_{CREF} = I_{REF} \times R$.

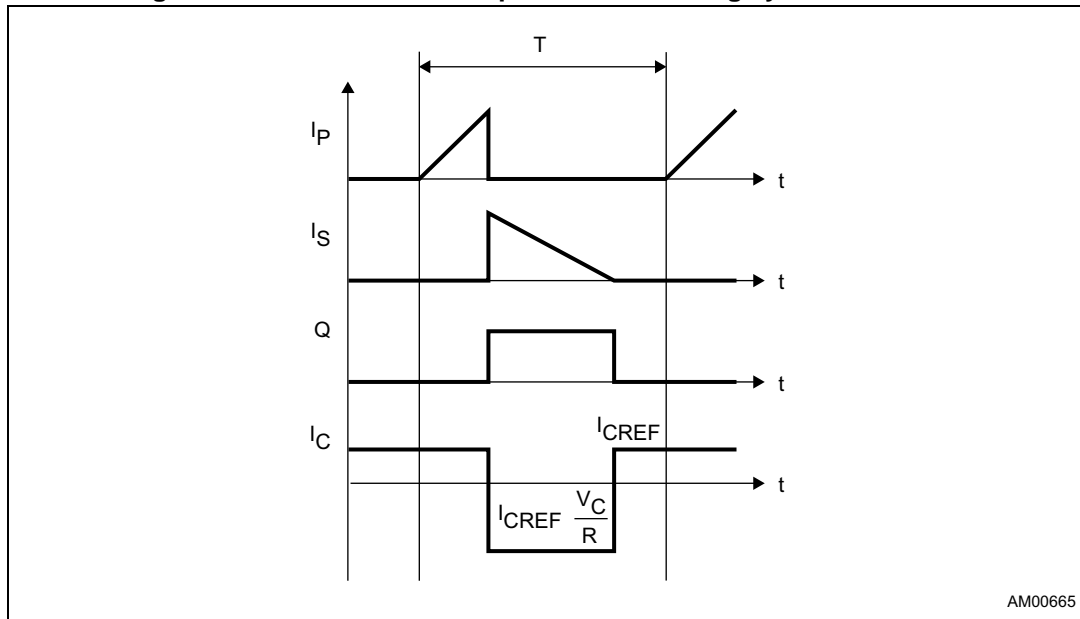
Equation 5 shows that the average output current no longer depends on input or output voltage, nor on the transformer inductance values. The parameters defining the output current are the transformer ratio n and the sense resistor R_{SENSE} , while the current reference voltage V_{CREF} (equal to $I_{REF} \times R$) is internally defined.

Figure 22. Current control principle



AM00666

Figure 23. Constant current operation: switching cycle waveforms



A.3 Current comparator speed

The propagation delay of the internal current comparator used in the CC control block causes the MOSFET to be switched off with a peak current higher than the theoretical value: this current overshoot is dependent on the input voltage and introduces an error in the calculated CC setpoint, rendering [Equation 5](#) no longer valid.

In order to make the cycle-by-cycle current limitation and the CC setpoint almost independent of the input voltage, a feed-forward function has been implemented, according to the schematic in [Figure 24](#).

During the MOSFET's ON-time, the current sourced from the ZCD/FB pin is mirrored inside the "feed-forward logic" block to provide the feed-forward current, I_{FF} .

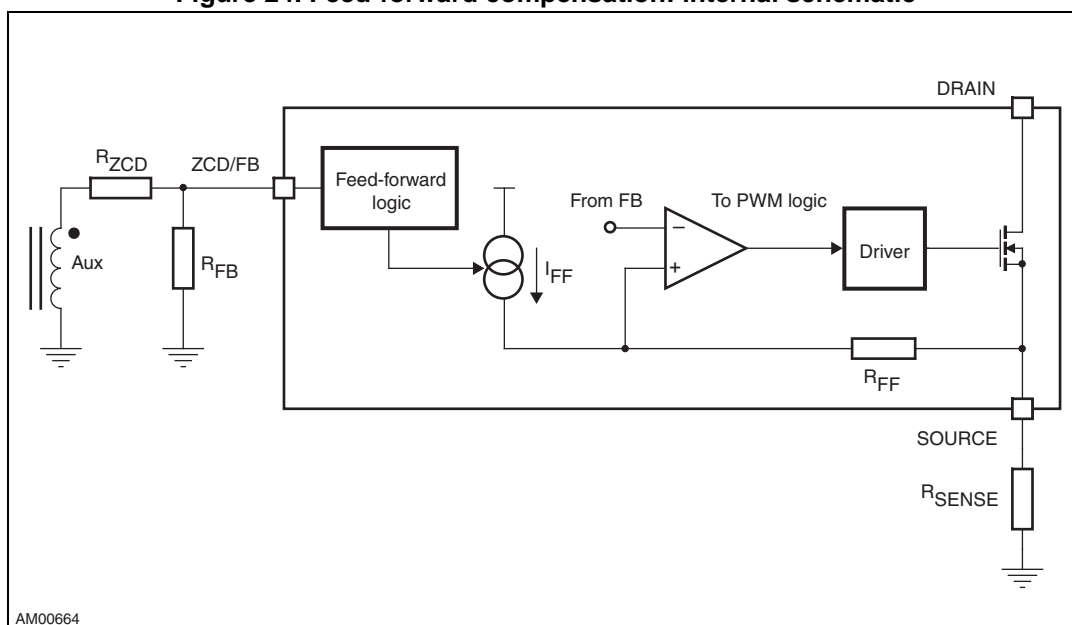
This feed-forward current is proportional to the input voltage and provides an offset on the current sense to compensate the propagation delay of the current comparator.

In order to achieve full compensation, the R_{ZCD} resistor should be selected based on the following equation:

Equation 6

$$R_{ZCD} = \frac{n_{AUX}}{n_{PRI}} \times \frac{L_P \times R_{FF}}{T_d \times R_{SENSE}}$$

Figure 24. Feed-forward compensation: internal schematic



A.4 Cable drop compensation block

The cable drop compensation (CDC) function is used to compensate the voltage drop across an output cable. In fact, the voltage on the end of the cable is lower than that at the beginning, depending on the output current level. This voltage drop may not be acceptable, especially in applications where tight voltage regulation is required and a long output cable is used.

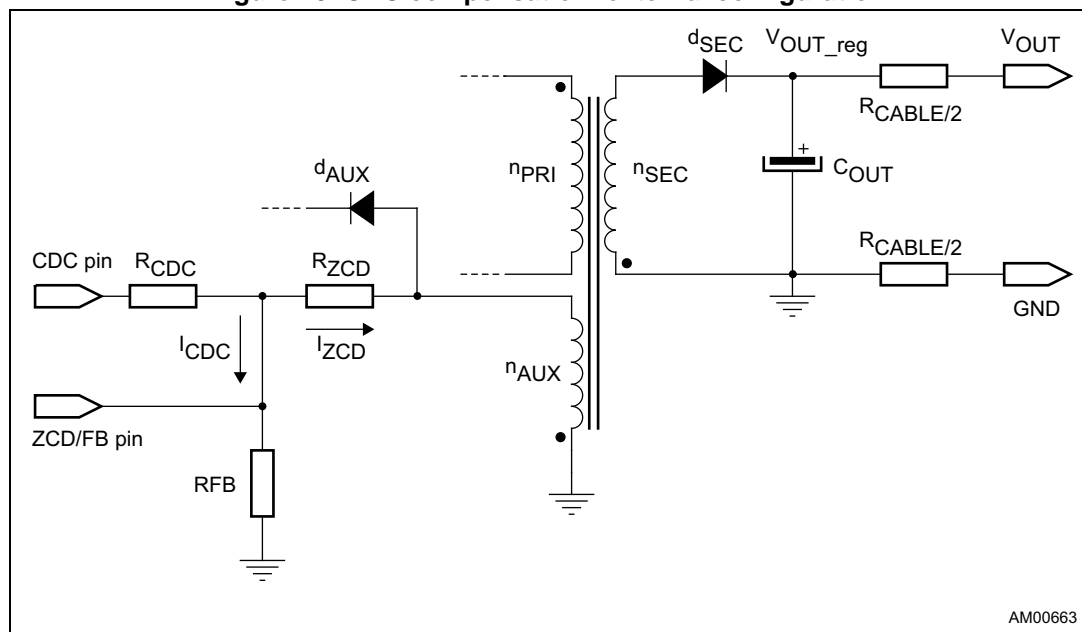
The CDC is a voltage source which provides, during constant voltage mode regulation, a voltage on the CDC pin lower than 2.5 V by an amount proportional to the output current.

According to [Figure 25](#), by connecting an appropriate resistor between this pin and the ZCD/FB pin, the CV setpoint is increased proportionally to I_{OUT} , so that the output at the end of the cable is almost constant. The R_{CDC} value can be calculated using [Equation 7](#):

Equation 7

$$R_{CDC} = \frac{2}{n} \times \frac{n_{SEC}}{n_{AUX}} \times \frac{R_{SENSE} \times R_{ZCD}}{R_{CABLE}}$$

Figure 25. CDC compensation: external configuration



AM00663

In [Equation 7](#), R_{CABLE} is the total resistance of the output cable.

The CDC block acts as a second-order correction and creates a positive feedback that can impact overall system stability. To avoid any issues that could render the loop unstable, the CV setpoint time response must be much lower than the main control signal. For this reason, the CDC block is designed with a time response of a few tens of milliseconds.

6 Revision history

Table 7. Document revision history

Date	Revision	Changes
21-Jul-2010	1	Initial release.
24-Feb-2016	2	Modified: Figure 2 .

IMPORTANT NOTICE – PLEASE READ CAREFULLY

STMicroelectronics NV and its subsidiaries ("ST") reserve the right to make changes, corrections, enhancements, modifications, and improvements to ST products and/or to this document at any time without notice. Purchasers should obtain the latest relevant information on ST products before placing orders. ST products are sold pursuant to ST's terms and conditions of sale in place at the time of order acknowledgement.

Purchasers are solely responsible for the choice, selection, and use of ST products and ST assumes no liability for application assistance or the design of Purchasers' products.

No license, express or implied, to any intellectual property right is granted by ST herein.

Resale of ST products with provisions different from the information set forth herein shall void any warranty granted by ST for such product.

ST and the ST logo are trademarks of ST. All other product or service names are the property of their respective owners.

Information in this document supersedes and replaces information previously supplied in any prior versions of this document.

© 2016 STMicroelectronics – All rights reserved